PHYSICAL REVIEW D **90,** 125016 (2014)

# Spontaneous *CP* violating quark scattering from asymmetric $Z(3)$ interfaces in the quark-gluon plasma

Abhishek Atreya,[*] Partha Bagchi,[†] Arpan Das,[‡] and Ajit M. Srivastava[§]

*Institute of Physics, Bhubaneswar 751005, India*

(Received 28 June 2014; published 17 December 2014)

In this paper, we extend our earlier study of the spontaneous *CP* violating scattering of quarks and antiquarks from QCD $Z(3)$ domain walls for the situation when these walls have asymmetric profiles of the Polyakov loop order parameter $l(x)$. Dynamical quarks lead to the explicit breaking of $Z(3)$ symmetry, which lifts the degeneracy of the $Z(3)$ vacua arising from spontaneous breaking of the $Z(3)$ symmetry in the quark-gluon plasma phase. The resulting domain walls have an asymmetric profile of $l(x)$ (under the reflection $x \to -x$ for a domain wall centered at the origin). We calculate the background gauge field profile $A_0$ associated with this domain wall profile. Interestingly, even with the asymmetric $l(x)$ profile, quark-antiquark scattering from the corresponding gauge field configuration does not reflect this asymmetry. We show that the expected asymmetry in scattering arises when we include the effect of the asymmetric profile of $l(x)$ on the effective mass of quarks and antiquarks and calculate the resultant scattering. We discuss the effects of such asymmetric $Z(3)$ walls in generating quark and antiquark density fluctuations in cosmology, and in relativistic heavy-ion collisions, e.g., event-by-event baryon fluctuations.

DOI: 10.1103/PhysRevD.90.125016 PACS numbers: 25.75.-q, 11.27.+d, 12.38.Mh

## I. INTRODUCTION

Search for the quark-gluon plasma (QGP) phase of QCD in relativistic heavy-ion collision experiments (RHICE) has reached a mature stage, with observations providing compelling evidence that the QGP phase is created in these experiments. While a definitive conclusion about the discovery of QGP is still awaited, it is an appropriate time to explore new effects and new structures in this exotic phase of QCD. This is particularly important due to its implications for the case of the early Universe, as well as for the cores of dense astrophysical objects like neutron stars. One such new effect is the possibility of extended topological objects in the QGP phase which arise from the spontaneous breaking of the center symmetry $Z(3)$ of the color $SU(3)$ group. The $Z(3)$ symmetry is broken spontaneously as the Polyakov loop, $l(x)$, which is an order parameter for the confinement-deconfinement phase transition for pure gauge theory [1], assumes a nonzero value in the deconfined phase. The resulting domain walls, so-called $Z(3)$ walls [2–4], are in some sense similar to the axionic domain walls in the Universe. Interestingly, just like axionic cosmic strings, here also there are topological strings associated with the junctions of these $Z(3)$ walls [5]. The study of these defects becomes more relevant in the present era of relativistic heavy-ion collision experiments as the temperature and energy densities that are needed to form these defects is (hopefully) accessible in these accelerators. In fact, these defects are the only defects in a relativistic quantum field theory that can be probed in present day laboratory conditions.

In earlier works, some of us have studied the formation and evolution of these topological objects in the initial transition to the QGP phase in the context of RHICE [6]. Various consequences of $Z(3)$ walls have been discussed in these works for RHICE arising from the nontrivial scattering of quarks from $Z(3)$ walls. Implications of the existence of these walls in the early Universe has also been discussed in [7], where it is shown that baryon inhomogeneities can arise from the scattering of quarks from $Z(3)$ walls. Scattering of quarks/antiquarks was studied in [7] by modeling the dependence of effective quark mass on the magnitude of the Polyakov loop order parameter $l(x)$. Spatial dependence of the profile of $l(x)$ leads to spatially varying effective mass, which behaves as potential in the Dirac equation for quarks/antiquarks leading to nontrivial scattering. As this effective mass (potential) is the same for quarks and antiquarks, the resulting scattering is the same for both.

In [8] we followed a different method for studying the scattering of quarks/antiquarks from $Z(3)$ walls. We assume that the profile of $l(x)$ corresponds to a sort of condensate of the background gauge field $A_0$ (following the definition of the Polyakov loop order parameter). We calculate this profile of the background gauge field from the profile of $l(x)$. Such a gauge field configuration, when used in the Dirac equation, leads to a potential which is different for quark and antiquark, leading to spontaneous *CP* violation in the scattering of quarks and antiquarks from a given $Z(3)$ wall. This *CP* violation is spontaneous,

[*]atreya@iopb.res.in
[†]partha@iopb.res.in
[‡]arpan@iopb.res.in
[§]ajit@iopb.res.in

 

as it arises from a specific background configuration of the gauge field corresponding to a given $Z(3)$ wall. This was first discussed by Altes *et al.* [9,10], who argued, in the context of the Universe, that due to the nontrivial background field configuration for the standard model gauge fields, the localization of quarks and antiquarks on the wall is different. Its possible effects on the electroweak baryogenesis via sphalerons was discussed in [9,10]. This spontaneous $CP$ violation for the case of QCD was also discussed in [11]. The $CP$ violating effects discussed in the above works were primarily qualitative, as the exact profiles of $A_0$ were not calculated. In [8], we use the profile of Polyakov loop $l(x)$ between different $Z(3)$ vacua [which was obtained by using the specific effective potential for $l(x)$, as discussed in [12]] to obtain the full profile of the background gauge field $A_0$. This background $A_0$ configuration acts as a potential for quarks and antiquarks, causing a nontrivial reflection of quarks from the wall. There we also showed that this spontaneous $CP$ violation arising from the background $A_0$ configuration leads to different reflection coefficients for quarks and antiquarks. In a series of follow-up works [13,14], we studied the effect of this difference on the scattering of quarks and antiquarks from $Z(3)$ walls in the context of ongoing relativistic heavy-ion collision experiments and the early Universe. In [13], we discussed a novel mechanism of $J/\psi$ disintegration in the relativistic heavy-ion collision experiments. We showed that the localized electric field in the $CP$ violating $Z(3)$ domain wall in the QGP phase leads to the disintegration of quarkonia. In [14], we studied the effect of this $CP$ violation on baryon transport across the collapsing $Z(3)$ domain walls in the early Universe. We showed that it can lead to the formation of quark nuggets as well as antiquark nuggets by segregating baryons and antibaryons in different regions of the Universe near a QCD phase transition epoch. As quarks are concentrated in a given collapsing domain wall, similar amounts of antiquarks get concentrated in another collapsing domain wall which has the $CP$ conjugate configuration of $A_0$ corresponding to the interchange of the two $Z(3)$ vacua with respect to the first domain wall case. Thus, for a given size of collapsing domain walls, the resulting nugget sizes are identical for quarks and antiquarks.

There have been some objections concerning the existence of $Z(3)$ walls (and of the associated field $A_0$) in the Minkowski space. We refer to our earlier work [8] for a discussion of this aspect. The existence of these $Z(3)$ walls becomes a nontrivial issue in the presence of quarks. It has been argued that $Z(3)$ symmetry loses its meaning in the presence of dynamical quarks [15,16]. It is argued there that these $Z(3)$ domains have unacceptable thermodynamic behavior, leading to negative specific heat and, more seriously, negative entropy. We recognize that there are certainly conceptual issues regarding the existence of these structures. However, at the same time they allow very interesting possibilities for the QGP phase, with rich phenomenology. It therefore looks reasonable to explore the possible consequences of these $Z(3)$ domains and associated walls. We may point out that despite these conceptual issues, amongst all models allowing for existence of topological extended structures (domain walls, strings, etc., which have been proposed in various particle physics theories in the early Universe), these $Z(3)$ domain walls (and the associated QGP string) may be most well motivated. Indeed, if these objects exist, these will be the only relativistic field theory topological solitons which are accessible in laboratory experiments. Their detection will not only provide deep insights into the nontrivial physics of the QGP phase, it will also have very important implications for cosmology.

We will follow the approach that one can regard the effect of quarks in terms of the explicit breaking of $Z(3)$ symmetry [17–19]. This finds support in the recent lattice calculations of QCD with quarks [20], which suggest that there is a strong possibility of the existence of these $Z(3)$ vacua at high temperatures. Since the presence of quarks lifts the degeneracy of different $Z(3)$ vacua, the $Z(3)$ interfaces are no longer solutions of time independent field equations as they move away from the region with the unique true vacuum. However, it is important to note that with quark effects (taken in terms of explicit symmetry breaking), the interfaces survive as nontrivial topological structures, even though they do not remain solutions of time independent equations of motion. As the resulting profile of $l(x)$ between the true vacuum and a metastable vacuum is no more symmetric, it raises interesting possibilities for the generation of quark and antiquark inhomogeneities as a network of collapsing domain walls is considered, with different walls interpolating between different sets of $Z(3)$ vacua. The situation is even more interesting, as with explicit symmetry breaking certain closed domain walls with a true vacuum inside (and with sufficiently larger size) may expand [21]. This can lead to the concentration of quarks and antiquarks in a shell-like structure, which can have important implications in cosmology (for large shells) and in RHICE, where it may imply a concentration of baryons or antibaryons near the surface of the QGP region.

With these motivations, we extend our earlier study of [8] in this paper with an incorporation of the effects of explicit symmetry breaking arising from dynamical quarks. We find that even though the profile of $l(x)$ is asymmetric in this case (under the reflection $x \to -x$), quark-antiquark scattering from the gauge field configuration associated with it does not show any difference from the symmetric case when explicit $Z(3)$ symmetry breaking is absent. More precisely, the scattering of a quark from true vacua on the wall is identical to the scattering of an antiquark from the metastable one. We then include the effect of the asymmetric profile of $l(x)$ on the effective mass of quarks and antiquarks and calculate resultant scattering. Because of the

asymmetric profile of $l(x)$, the resulting effective mass of quarks and antiquarks is different when considering the scattering of the quark coming from the true vacua or from the metastable one (though it is the same for quark and antiquark). This, combined with the *CP* violating scattering resulting from the background gauge field configuration associated with this $l(x)$, leads to asymmetry in the scattering of quarks moving from the true vacuum towards the metastable vacuum and antiquarks moving from the metastable vacuum towards the true vacuum. This will lead to important differences in the resulting concentrations of quarks and antiquarks in cosmology as well as in RHICE. In our entire discussion we have assumed that the true vacua is on the left of the domain wall, while the metastable one is on the right.

The paper is organized in the following manner. In Sec. II we recall the basic physics of the origin of spontaneous *CP* violation due to the presence of $Z(3)$ interfaces and briefly introduce the effective potential for the Polyakov loop incorporating the explicit breaking of $Z(3)$ symmetry. Calculation of the *asymmetric* profile of $l(x)$ for this case and its associated gauge field configuration is somewhat nontrivial and we discuss this in Sec. III. In Sec. IV we first discuss the scattering of quarks and antiquarks from this gauge field configuration and show that it leads to the same results for quark and antiquark concentrations as for the case without any explicit symmetry breaking. We then introduce the $l(x)$ dependent effective mass for quarks and antiquarks and show that the resultant scattering is different for quarks moving from true vacuum towards the metastable vacuum and antiquarks moving from metastable vacuum towards the true vacuum. Section V presents a discussion and conclusions where we discuss the possible implications of these results for cosmology and RHICE.

## II. SPONTANEOUS *CP* VIOLATION FROM $Z(3)$ WALLS

We briefly recall the basic physics of the origin of the spontaneous *CP* violation arising from $Z(3)$ walls. The source of this *CP* violation is a background condensate of the gauge field $A_0$ which we take to correspond to the profile of $l(x)$. This association is made following the definition of the Polyakov loop [1,22,23],

$$L(x) = \frac{1}{N}\mathrm{Tr}\left[\mathbf{P}\exp\left(ig\int_0^\beta A_0(\vec{x},\tau)d\tau\right)\right], \qquad (1)$$

where $A_0(\vec{x},\tau) = A_0^a(\vec{x},\tau)T^a, (a = 1,\ldots N)$ are the gauge fields and $T^a$ are the generators of $SU(N)$ in the fundamental representation. $\mathbf{P}$ denotes the path ordering in the Euclidean time $\tau$, and $g$ is the gauge coupling. Under the global $Z(N)$ symmetry transformation, the Polyakov loop transforms as

$$L(x) \longrightarrow Z \times L(x), \quad \text{where } Z = e^{i\phi}, \qquad (2)$$

with $\phi = 2\pi m/N$; $m = 0, 1\ldots(N-1)$.

The thermal average of the Polyakov loop, $\langle L(x)\rangle$ [which we denote as $l(x)$], is related to the free energy of an infinitely heavy test quark in a pure gluonic medium [$l(x) \propto e^{-\beta F}$]. In the confined phase, a test quark should have infinite energy implying that $l(x) = 0$. In the deconfined phase, a test quark will have finite energy, implying a nonzero value of $l(x)$. Thus $l(x)$ serves as an order parameter for the confinement-deconfinement transition. In view of Eq. (2), a nonzero value of $l(x)$ leads to a spontaneous breaking of the $Z(N)$ symmetry in the high temperature deconfined phase, while this symmetry is restored in the low temperature confined phase when $l(x) = 0$. For QCD, $N = 3$, hence, the confinement-deconfinement transition in QCD corresponds to a spontaneous breaking of $Z(3)$ symmetry leading to the $Z(3)$ domain walls (and the associated QGP string; see Ref. [5]).

As we mentioned, we determined the background gauge field configuration $A_0$ from the profile of $l(x)$ for a specific domain wall which interpolates between two $Z(3)$ vacua without quark effects. For determining the profile of $l(x)$ interpolating between different $Z(3)$ vacua, we used the specific effective potential for the Polyakov loop from Ref. [12], with the Lagrangian density given by

$$L = \frac{N}{g^2}|\partial_\mu l|^2 T^2 - V(l). \qquad (3)$$

Here $N = 3$ for QCD. $T^2$ is multiplied in the first term to give the correct dimensions to the kinetic term. The effective potential $V(l)$ for the Polyakov loop is given as

$$V(l) = \left(-\frac{b_2}{2}|l|^2 - \frac{b_3}{6}(l^3 + (l^*)^3) + \frac{1}{4}(|l|^2)^2\right)b_4 T^4. \qquad (4)$$

The coefficients $b_2$, $b_3$, and $b_4$ are dimensionless quantities. These parameters are fitted in Refs. [17–19] such that the effective potential reproduces the thermodynamics of pure $SU(3)$ gauge theory on a lattice [24,25]. The coefficients are $b_2 = (1 - 1.11/x)(1 + 0.265/x)^2(1 + 0.300/x)^3 - 0.478$ (with $x = T/T_c$ and $T_c \sim 182$ MeV), $b_3 = 2.0$, and $b_4 = 0.6061 \times 47.5/16$. With these values, $l(x) \longrightarrow y = b_3/2 + \frac{1}{2}\times\sqrt{b_3^2 + 4b_2(T=\infty)}$ as $T \longrightarrow \infty$. Various quantities are then rescaled such that $l(x) \longrightarrow 1$ as $T \longrightarrow \infty$. The scalings are

$$l(x) \to \frac{l(x)}{y}, \qquad b_2 \to \frac{b_2}{y^2},$$
$$b_3 \to \frac{b_3}{y}, \qquad b_4 \to b_4 y^4. \qquad (5)$$

At low temperatures where $l = 0$, the potential has only one minimum. For temperatures higher than $T_c$, the Polyakov loop develops a nonvanishing vacuum expectation value $l_0$, and the cubic term above leads to $Z(3)$ degenerate vacua. The $l(x)$ profile is calculated by energy

minimization; see Ref. [5] for details. From the $l(x)$ profile, the $A_0$ profile is calculated by inverting Eq. (1). Figure 1 shows the $|l(x)|$ profile as obtained by a minimization of energy. This is the red (solid) curve on the left figure. We then calculate the $A_0$ profile from the $l(x)$ profile, which is shown on the right in Fig. 1. This $A_0$ profile was then used to calculate $|l(x)|$ again to see if it reproduces the $|l(x)|$ as given by the energy minimization program. Cal $|L|$ (dashed curve) in the left figure shows the profile calculated from $A_0$. The inset shows the error between two $|L|$ values, clearly showing that our method works very well.

For various conceptual issues regarding this calculation, we refer to our earlier work [8]. To address the issue of uncertainties in the determination of the $A_0$ profile depending on the choice of the specific form of the effective potential, we had repeated this calculation of $A_0$ profile, in Ref. [8], for another choice of an effective potential of the Polyakov loop, as provided by Fukushima [26]. It was found that even though the two effective potentials (in Refs. [12] and [26]) are of qualitatively different shapes, the resulting wall profile and the $A_0$ profile were very similar. This gives us confidence that our conclusions arising from the calculations of the scattering of quarks and antiquarks from $Z(3)$ walls are not crucially dependent on the specific choice of the effective potential.

We now include the effects of dynamical quarks leading to an explicit breaking of $Z(3)$ symmetry. For this, we will follow the approach where the explicit breaking of the $Z(3)$ symmetry is represented in the effective potential by inclusion of a linear term in $l$ [17–19,27]. The above potential $V(l)$ with the linear term becomes

$$V(l) = \left(-\frac{b_1}{2}(l + l^*) - \frac{b_2}{2}|l|^2 - \frac{b_3}{6}(l^3 + l^{*3}) + \frac{1}{4}(|l|^2)^2\right) b_4 T^4. \quad (6)$$

Here coefficient $b_1$ measures the strength of explicit symmetry breaking. [In view of Eq. (5), $b_1$ is scaled as $b_1 \to b_1/y^3$.] A discussion of various values that $b_1$ can have is given in [27]. A nonzero value of $b_1$ lifts the degeneracy between the three $Z(3)$ vacua. Vacua corresponding to $\theta = 2\pi/3$ $(l = z)$ and $\theta = 4\pi/3$ $(l = z^2)$ remain degenerate, while the true vacuum with a lower energy corresponds to $l = 1$ $(\theta = 0)$. Thus, the $l = z$ and $l = z^2$ vacua become metastable. The value of $b_1$ can be related to the estimates of explicit $Z(3)$ symmetry breaking arising from quark effects which have been discussed in the literature. In the high temperature limit, the estimate of the difference in the potential energies of the $l = z$ vacuum and the $l = 1$ vacuum, $\Delta V$, is given in Ref. [28] as

$$\Delta V \sim \frac{2}{3}\pi^2 T^4 \frac{N_l}{N^3}(N^2 - 2), \quad (7)$$

where $N_l$ is the number of massless quarks. If we take $N_l = 2$, then $\Delta V \simeq 3T^4$. For $T = 400$ MeV, this value of $\Delta V$ is obtained if we take the value of $b_1 = 0.645$. For temperatures of order $T_c$, it is not clear what should be the appropriate value of $b_1$. It is entirely possible that $b_1$ may be very small near $T_c$. (Possible reasons for taking very small values of $b_1$ are discussed in detail in Ref. [21].) We mention that as the parameter values for the effective potential [Eq. (6)] are appropriate for $T$ near $T_c$, we confine our attention to temperatures between $T_c$ and 400 MeV (as a sample value). This is also the regime of the temperature of interest for heavy-ion collisions and for baryon inhomogeneity generation before the quark-hadron transition in the Universe. For such temperatures, the number of massless quarks $N_l = 2$ looks appropriate. This already gives a very large value of $\Delta V$, as mentioned above (compared to the central barrier height of the effective potential, as explained in detail in Refs. [5–7]). $N_l = 3$ will give an even larger value of $\Delta V$, leading to a somewhat larger value of $b_1$. The smallest value of $b_1$ we consider to be 0.03 as a sample value for small explicit symmetry breaking. Such values were considered in Ref. [21], as with small explicit symmetry breaking there is a range of temperatures where a first order transition happens. For large values of $b_1$, the

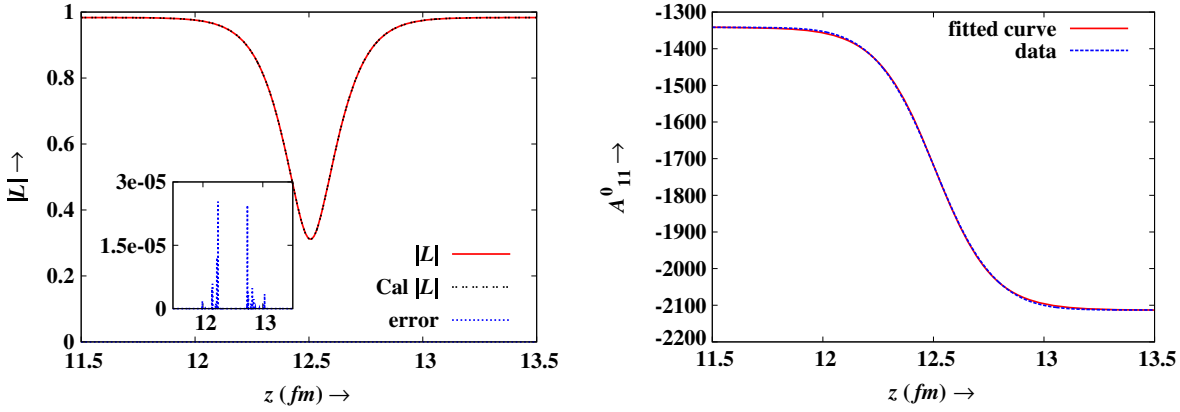


FIG. 1 (color online). Plot of $|l(x)|$ obtained from an energy minimization for $b_1 = 0.0$ and $T = 400$ MeV. The corresponding $A_0$ configuration is on the right. The $A_0$ profile fits well with a tanh function.

first order transition disappears. In view of these uncertainties in the magnitude of explicit symmetry breaking for temperatures near $T_c$, we will consider a range of values of $b_1$ between 0.03–0.65. This range seems large enough to illustrate the basic physics of how asymmetry of the wall affects the reflection coefficients. We determine the profile of $l(x)$ and the associated $A_0$ profile for these values of $b_1$.

## III. PROFILES OF $l(x)$ AND ASSOCIATED GAUGE FIELD CONFIGURATION WITH EXPLICIT SYMMETRY BREAKING

The explicit symmetry breaking arising from quark effects will have important effects on the structure of $Z(3)$ walls. For nondegenerate vacua, even planar $Z(3)$ interfaces do not remain static and move away from the region with the unique true vacuum. Thus, while for the degenerate vacua case every closed domain wall collapses, for the nondegenerate case this is not true anymore. A closed wall enclosing the true vacuum may expand if it is large enough so that the surface energy contribution does not dominate.

The absence of time independent solutions of the field equations for $Z(3)$ walls leads to complications in the implementation of the techniques of Ref. [5] for a determination of the $l(x)$ profile for the domain wall which was based on the algorithm of energy minimization. In Ref. [5], the correct $l(x)$ profile was obtained from an initial trial profile by fluctuating the value of $l(x)$ at each lattice point and determining the acceptable fluctuation which lowers the energy (with suitable overshoot criterion, etc., as described in detail in Ref. [5]). For the case without explicit symmetry breaking, a trial initial configuration of $l(x)$ with appropriate fixed boundary conditions [corresponding to the two $Z(3)$ vacua under consideration] yielded the correct profile of $l(x)$ for the wall within relatively few iterations. However, with explicit symmetry breaking, this simple procedure fails, as energy can always be lowered by shifting the wall towards metastable vacua (thus expanding the region with a true vacuum).

From the computational point of view, one of the major changes due to the inclusion of the $b_1$ term is the scaling. Without $b_1$, all of the vacua are degenerate, so $|l(x)| \to 1$ in all of the vacua. However, that is not the case with the potential given by Eq. (6). This leads to the $b_1$ dependence of the scaling. We normalize the potential in such a manner that $|l(x)| \to 1$ in the true vacuum. As we mentioned above, the energy splitting between vacua itself amounts to a pressure difference between the two vacua. Thus the program tries to minimize the energy by moving the domain wall in one direction till it goes completely out of the lattice; in the process it changes the boundary values too if they are not held fixed. If we fix the boundary value in the far left and far right region of the lattice, the program minimizes the energy by not only moving the profile in the intermediate region but also by readjusting the values of $|l(x)|$ on the two sides. The effect is most pronounced for the large $b_1$. This statement becomes clearer if we look at Fig. 2. It shows the initial and final profiles of $l(x)$ between the $l = 1$ and $l = z$ vacua for $b_1 = 0.645$ at $T = 400$ MeV. The asymmetry is pretty clear in the boundary conditions of the initial trial configuration itself. Note the central region in the final configuration (the solid curve). There is a sharp variation of $|l(x)|$ in a small region and on either side of it the $|l(x)|$ values are the same (but different from actual boundary values), leading to a stable configuration in the middle. Since the domain wall is characterized by the sharp variation of the field in a small spatial region, we fit the profile such that it meets the correct boundary values while keeping the variation as given by the energy minimization program. This is shown by the dotted curve in the left figure. Though this procedure of a *smoothening* of the domain wall profile near its edges is somewhat *ad hoc*, it will not affect our results much, as the scattering of quarks and antiquarks is primarily decided by the height and width of the sharply varying profile of $l(x)$. Upon comparison

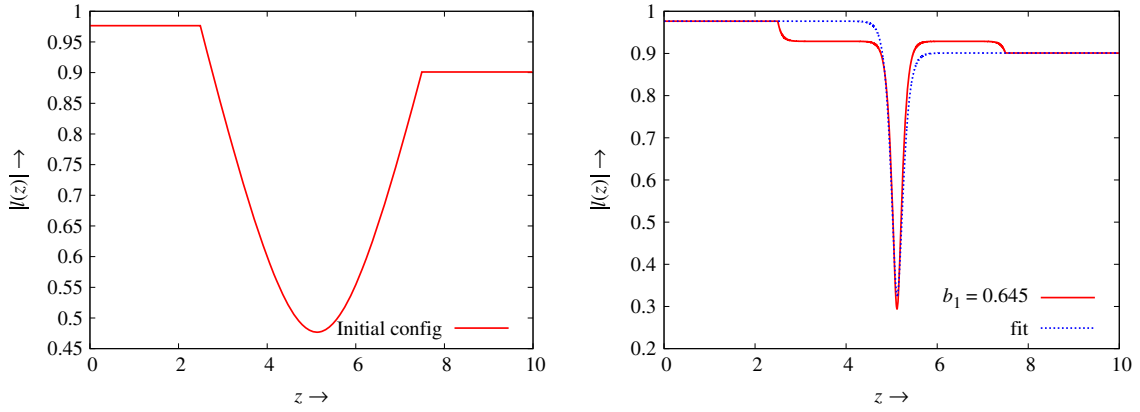


FIG. 2 (color online). Plot of $|l(x)|$ obtained from the energy minimization for $b_1 = 0.645$ (the solid curve). On the left is the initial trial configuration. The final configuration is on the right.

with Fig. 1 (for the $b_1 = 0$ case), we note that the explicit breaking of the $Z(3)$ symmetry leads to asymmetric profiles of $l(x)$. This immediately suggests that there will be a difference between the scattering of a quark coming from the right (from the metastable vacuum side) and the scattering of the one coming from the left (from the true vacuum side).

The $A_0$ profile corresponding to the $l(x)$ profile was calculated in our earlier paper [8], where we also discussed various conceptual issues related to the ambiguities in the extraction of a colored quantity $A_0$ from color singlet $l(x)$. We choose the Polyakov gauge (diagonal gauge) for $A_0$:

$$A_0 = \frac{2\pi T}{g}\left(a\frac{\lambda_3}{2} + \frac{b\lambda_8}{2}\right), \tag{8}$$

where $g$ is the coupling constant and $T$ is the temperature, while $\lambda_3$ and $\lambda_8$ are the diagonal Gell-Mann matrices. The $A_0$ profile was obtained from the $l(x)$ profile (Fig. 2) by inverting Eq. (1). We present a brief discussion of how to obtain the $A_0$ profile from the $l(x)$ profile. See Ref. [8] for details. Substituting Eq. (8) into Eq. (1) and comparing the real and imaginary parts, we get

$$\cos(\alpha) + \cos(\beta) + \cos(\gamma) = 3|l(x)|\cos(\theta), \tag{9a}$$

$$\sin(\alpha) + \sin(\beta) + \sin(\gamma) = 3|l(x)|\sin(\theta), \tag{9b}$$

where, $\alpha = 2\pi(a+b)$, $\beta = 2\pi(b-a)$, and $\gamma = 2\pi(-2b)$ [(a,b) are defined in Eq. (8)]. $\theta$ is defined by $l(x) = |l(x)|e^{i\theta}$. For each of the $l = 1, z, z^2$ vacua, the solutions are a set of the ordered pairs $(a,b)_{L=1,z,z^2}$. We choose one pair, $(a,b)_{L=1}$, as the initial condition. By demanding that $a$ and $b$ (and hence $A_0$) vary smoothly across the wall [as the profile of $L(x)$ changes smoothly], we approach the appropriate values of $(a,b)_{L=z}$ in the $L = z, z^2$ vacuum. Once we have the $a$ and $b$ profiles, $A_0$ is calculated using Eq. (8). We have carried out this calculation for the profiles of $l(x)$ obtained from the energy minimization program for $b_1 \neq 0$ (Fig. 2). The calculated $a, b$ was then used to calculate $A_0$ using Eq. (8). The $A_0$ profile thus obtained is reasonably well fitted to the function $A_0(x) = p\tanh(qx + r) + s$ using GNUPLOT. The calculated $A_0$ profile and the fitted $A_0$ profile are plotted in Fig. 3.

We note that the fit to the tanh profile is almost perfect, just as in the case of $b_1 = 0$ in Fig. 1. We thus conclude that the scattering of a quark coming from the side of a true vacuum with such an $A_0$ profile (in the Dirac equation) will be the same as the scattering of an antiquark coming from the side of the metastable vacuum (with the same kinetic energy). Thus a collapsing domain wall with $l = 1$ inside and $l = z$ outside will give the same reflection coefficients (and hence the same resulting concentration) for quarks inside as a collapsing domain wall with $l = z$ inside and $l = 1$ outside will give for antiquarks (assuming zero baryon chemical potential). This is interesting in view of the asymmetric profiles of $l(x)$ in Fig. 2 for $b_1 \neq 0$ cases. There will still be important differences from the $b_1 = 0$ case, however, as now a sufficiently large closed domain wall with a true vacuum ($l = 1$) inside will expand instead of collapsing, leading to the concentration of quarks or antiquarks in a shell-like region. We will discuss these possibilities later in Sec. V.

It may also be noted that we have shown $A_0^{11}$ for $b_1 = 0.645$ and $A_0^{22}$ for $b_1 = 0.03$. This is because both of the profiles are similar in shape and size. It has to do with the choice of initial $(a,b)$ values while calculating $A_0$. When extracting $A_0$ from the $l(x)$ profile by inverting Eq. (1) using Eq. (8), we get various sets of values for $(a,b)$. We take one set as the initial condition and get the $A_0$ profile. Now if we take another value, say $(-a,b)$, then from Eq. (8) it is clear that $A_0^{11}$ and $A_0^{22}$ get interchanged. This means that whatever the reflection probability for the red quark in the first case was, it is the same for the green quark in the second case. That is the case in Fig. 3. This essentially means that we should compare the reflection of the red quark in the $b_1 = 0.645$ case with the reflection of the green quark in the $b_1 = 0.03$ case. One may use the hit and trial method to find a specific choice of $(a,b)$ in the

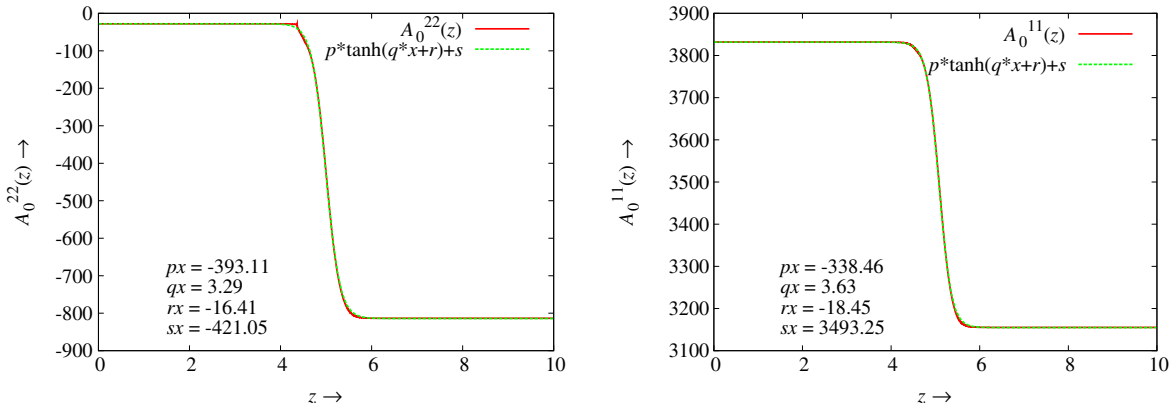


FIG. 3 (color online). Plot of the calculated $A_0$ and the fitted profile $[A_0(x) = p\tanh(qx + r) + s]$ for $b_1 = 0.03$ and 0.645.

case of $b_1 = 0.03$ such that the $A_0^{11}$ obtained has the same spatial variation as the one for $b_1 = 0.645$. We refer to Ref. [8] for further details on this issue of initial conditions. We would like to point out that there were typographical errors in Eq. (7), and in the definitions of $\alpha, \beta, \gamma$ in Eq. (8) in Ref. [8].

As we mentioned, it is interesting to note that the asymmetry of $l(x)$ is not reflected in the background gauge configuration. The effect of nonzero $b_1$ is reflected in the $A_0$ profile not in terms of the change in shape but in terms of the height of the potential getting reduced. For $b_1 = 0.645$, the height of $A_0$ is almost 100 MeV less than the height of $A_0$ in the $b_1 = 0.03$ case. However, this decrease in height will not give any asymmetry in the reflection of the quarks and antiquarks from the $A_0$; neither will it change the amount of reflection in a drastic fashion. We will now consider another possibility which allows for asymmetry in the concentration of quarks and antiquarks for the $b_1 \neq 0$ case.

For this we recall the discussion of quark/antiquark scattering due to $l$ dependent effective mass, as discussed in Ref. [7]. The basic idea proposed in Ref. [7] was that as $l(x)$ is the order parameter for the quark-hadron transition, physical properties such as the effective mass of the quarks should be determined in terms of $l(x)$. This also looks natural from the expected correlation between the chiral condensate and the Polyakov loop. Lattice results indicate that the chiral phase transition and the deconfinement phase transition may be coupled, i.e., as the Polyakov loop becomes non zero across $T_c$, the chiral order parameter attains a vanishingly small value. Thus, if there is a spatial variation in the value of $l(x)$ in the QGP phase, then the effective mass of the quark traversing that region should also vary (say, due to a spatially varying chiral condensate). For regions where $l(x) = 0$, quarks should acquire constituent mass as appropriate for the confining phase. To model the dependence of the effective quark mass on $l(x)$, we could use the color dielectric model of Ref. [29] identifying $l(x)$ with the color dielectric field $\chi$ in Ref. [29]. The effective mass of the quark was modeled in [29] to be inversely proportional to $\chi$. This leads to a divergent quark mass in the confining phase consistent with the notion of confinement. However, we know that the divergence of quark energy in the confining phase should be a volume divergence (effectively, the length of string connecting the quark to the boundary of the volume). $1/l(x)$ dependence will not have this feature; hence, we do not follow this choice. For the sake of simplicity and for order of magnitude estimates at this stage, we will model the quark mass dependence on $l(x)$ in the following manner:

$$m(x) = m_q + m_0(l_0 - |l(x)|). \tag{10}$$

Here $l(x)$ represents the profile of the $Z(3)$ domain wall, and $l_0$ is the vacuum value of $|l(x)|$ (for the true vacuum) appropriate for the temperature under consideration. $m_q$ is the current quark mass of the quark as appropriate for the QGP phase with $|l(x)| = l_0$, with $m_u \simeq m_d = 10$ MeV and $m_s \simeq 140$ MeV. $m_0$ characterizes the constituent mass contribution for the quark. We will take $m_0 = 300$ MeV. Note that here $m(x)$ remains finite even in the confining phase with $l(x) = 0$. As mentioned above, this is reasonable since we are dealing with a situation where $l(x)$ differs from $l_0$ only in a region of thickness of order 1 fm (thickness of the domain wall).

The space dependent part of $m(x)$ in Eq. (10) is taken as a potential term in the Dirac equation for the propagation of quarks and antiquarks. As we can see from Fig. 1, $l(x)$ varies across a $Z(3)$ interface, acquiring a small magnitude in the center of the wall. A quark passing through this interface, therefore, experiences a nonzero potential barrier leading to a nonzero reflection coefficient for the quark. The important thing here is that because of the asymmetric profile of $l$ (Fig. 2), the effective mass of the quarks/antiquarks will have different values on the two sides of the domain wall. This effect, when combined with the scattering from the background $A_0$ configuration, will lead to asymmetry in the scattering of the quarks from one side and that of the antiquarks from the other side of the domain wall.

One may be concerned here whether combining the scattering from the $A_0$ configuration with the scattering due to the $l$ dependent effective mass amounts to double counting, in the sense that both effects originate from the same $l(x)$ profile. For this we note that there are indeed two different effects at play here due to the existence of $Z(3)$ walls. The first effect arises from the existence of three different phases of the QGP characterized by the spontaneous breaking of $Z(3)$ symmetry. In the absence of explicit symmetry breaking one will expect that the physics should be identical for these three phases. Thus, even the $l$ dependent effective mass of quarks should have the same value in these three phases, as indeed is the case in Eq. (10) due to the same value of $|l|$ in the three $Z(3)$ phases. However, with explicit symmetry breaking, there is no physical argument to say that the physics should be the same for the three $Z(3)$ vacua, as the two vacua ($l = z$ and $l = z^2$) become metastable. As $|l|$ in these two vacua has a smaller magnitude, the effective mass of the quarks may actually be larger in these two phases of QGP. As explained for Eq. (10), we can think of this $|l|$ dependent mass in terms of a chiral condensate whose value will depend on $l(x)$. [We mention that the $l(x)$ dependent quark mass by itself is a nontrivial implication of our proposal and it will have many other interesting implications on the propagation of quarks/antiquarks in QGP in the presence of these $Z(3)$ domains.] Next we come to the presence of the background gauge field. This arises from a spatial variation of $l(x)$ leading to a color electric field from which quarks and antiquarks scatter in different manner. This color electric field is entirely localized at the boundary of

TABLE I. Table for the reflection coefficients $R_q$ for the charm quark and $R_{aq}$ for the charm antiquark for smooth profiles of $A_0$ and $m(x)$.

| | $b_1 = 0.03$ | 0.126 | 0.645 |
|---|---|---|---|
| true → metastable vacuum $R_q$ | $1.65437 \times 10^{-6}$ | $4.40706 \times 10^{-6}$ | $1.43314 \times 10^{-10}$ |
| metastable → true vacuum $R_q$ | 0.00003366 | 0.0141752 | 0.00394808 |
| true → metastable vacuum $R_{aq}$ | $2.25671 \times 10^{-6}$ | $1.85367 \times 10^{-7}$ | $2.07835 \times 10^{-7}$ |
| metastable → true vacuum $R_{aq}$ | 0.000376883 | 0.0820803 | 0.073885 |

$Z(3)$ domains [where $l(x)$ has a spatial variation] and vanishes in the interiors of the $Z(3)$ domains. It couples differently to quarks/antiquarks of different color charges. Hence, this effect is entirely different from the effect of an effective mass which has different values in the interiors of the two domains, irrespective of the color charges of quarks and antiquarks [even though for scattering purposes, both effects lead to a nontrivial potential at the location of the $Z(3)$ wall].

## IV. REFLECTION AND TRANSMISSION COEFFICIENTS WITH EXPLICIT SYMMETRY BREAKING

We now calculate the reflection and transmission coefficient for quarks and antiquarks subject to the above two effects. One is $CP$ violating, arising from the background gauge field $A_0$ [Eq. (8)], and the other is $CP$ preserving, arising from the space dependent effective mass of the quarks/antiquarks [Eq. (10)]. We recall the steps for calculation from [8]. To calculate the reflection and transmission coefficient, we need the solutions of the Dirac equation in the Minkowski space, but the $A_0$ profile is calculated in Euclidean space. We start with the Dirac equation in the Euclidean space, with the spatial dependence of $A_0$ calculated from the $Z(3)$ wall profile as mentioned above, and with the space dependent mass term as given in Eq. (10):

$$[\gamma_e^0 \partial_0 \delta^{jk} - g\gamma_e^0 A_0^{jk}(z) + (i\gamma_e^3 \partial_3 + m(x))\delta^{jk}]\psi_k = 0, \quad (11)$$

where $\gamma_e^0 \equiv i\gamma^0$ and $\gamma_e^3 \equiv \gamma^3$ are the Euclidean Dirac matrices. $\partial_0$ denotes $\partial/\partial_\tau$, with $\tau = it$ being the Euclidean time. $j, k$ denote color indices. $m(x)$ is the effective mass given in Eq. (10). We now analytically continue Eq. (11) to the Minkowski space to get

$$[i\gamma^0 \partial_0 \delta^{jk} + g\gamma^0 A_0^{jk}(z) + (i\gamma^3 \partial_3 + m(x))\delta^{jk}]\psi_k = 0, \quad (12)$$

where $\partial_0$ now denotes $\partial/\partial t$ in the Minkowski space.

Equation (12) is used to calculate the reflection and transmission coefficients. For a general smooth potential we followed a numerical approach given by Kalotas and Lee [30]. They have discussed a numerical technique to solve a Schrödinger equation with potentials having arbitrary smooth space dependence. We applied this technique of Ref. [30] for solving the Dirac equation (see Ref. [8] for details).

The results for the charm quark and the antiquark (with $E = 3.0$ GeV taken as the example for each case) are given in Table I. As we discussed above, the $A_0$ profile depends on the choice of $(a, b)$ [Eq. (8)]. Thus, to have a proper comparison of the effect of the values of $b_1$, it is important to have the most similar profiles possible for $A_0$ for the different choices of $b_1$. The profiles used for calculating the reflection coefficients in Table I corresponded to $A_0^{11}$ for $b_1 = 0.126$ and 0.645, while the profile of $A_0^{22}$ was used for $b_1 = 0.03$. As we mentioned, the important quantity for us to calculate is the reflection coefficient of (say) quarks moving from the true vacuum towards the metastable vacuum through the wall and compare it with the reflection coefficient of the antiquarks (with the same kinetic energy) moving from the metastable vacuum towards the true vacuum through the wall. Any (possible) difference in these two reflection coefficients directly relates to the expected concentration of quarks and antiquarks by a domain wall of one kind and its opposite wall [interpolating between the two $Z(3)$ vacua in reverse order]. Table I shows a clear difference in these two reflection coefficients.

## V. DISCUSSION

In this work we have extended our earlier studies of $CP$ violating scattering of quarks/antiquarks from $Z(3)$ walls [8,13,14] by including the effects of the explicit breaking of $Z(3)$ symmetry which is expected to arise due to dynamical quarks. The resulting profile of $l(x)$ between the true vacuum and a metastable vacuum is no more symmetric in this case, which leads to new effects. We study the scattering of quarks and antiquarks from the background $A_0$ field associated with the profile of $l(x)$ while also incorporating the effect of spatially varying the effective mass of quarks and antiquarks in the respective $Z(3)$ domains. The combined effect of the scattering shows interesting behavior leading to the asymmetry in the scattering of quarks moving from the true vacuum towards the metastable vacuum and antiquarks moving from the metastable vacuum towards the true vacuum. This will lead to important differences in the resulting concentrations of quarks and antiquarks in cosmology as well as in RHICE. For example, in the early Universe, a network of domain walls will arise with varying sizes and interpolating between different $Z(3)$

vacua. For all domain walls of a given size interpolating between two given vacua in a given order, there will be roughly the same number of walls with a similar size but interpolating between the same two $Z(3)$ vacua in the reverse order (though explicit symmetry breaking may also produce differences between the formation of such walls, introducing further richness in the effects of explicit symmetry breaking). In the absence of explicit symmetry breaking, if the first type of walls gives a certain concentration of (say) quarks, then the other set of walls will give a similar concentration of antiquarks. This is, however, not the case when explicit symmetry breaking effects are incorporated. In view of the results from Table I, the two sets of walls will lead to very different concentrations of quarks and antiquarks (especially if the value of $b_1$ is large). Though for each domain wall (say, interpolating between $l = 1$ and $l = z$), there is always the *conjugate* wall (interpolating between $l = 1$ and $l = z^2$) which will lead to the same scattering between quarks and antiquarks. The final effect of our results will then appear as two different magnitudes for the concentrations of quarks and antiquarks, even if one takes all of the domain walls of the same size. This is very different from the case without explicit symmetry breaking where domain walls of same size will lead to quark and antiquark inhomogeneities of the same magnitude (for the same kinetic energies of quarks and antiquarks). This difference will be particularly dramatic for RHICE, where the number of domain walls is of order 1 for each event [6]. Thus even for the same type of events, one may get a very different concentration of baryons or antibaryons in different events, leading to very large event-by-event fluctuations.

The situation is even more interesting when we consider the effect that with explicit symmetry breaking, certain closed domain walls may expand—those with a true vacuum inside (and with sufficiently larger size so that the volume energy difference dominates over the surface energy contribution [21]). This can lead to the concentration of quarks and antiquarks in a shell-like structure. For cosmology, very large expanding domain walls may trap shells of baryons/antibaryons if enclosed by a collapsing *antiwall* configuration. Such shells can form in RHICE also and will have important observation signatures.

## ACKNOWLEDGMENTS

We are extremely thankful to Shreyash Shankar Dave, Sanatan Digal, and Saumia P. S. for the fruitful discussions.

[1] A. M. Polyakov, Phys. Lett. **72B**, 477 (1978).
[2] T. Bhattacharya, A. Gocksch, C. Korthals Altes, and R. D. Pisarski, Nucl. Phys. **B383**, 497 (1992).
[3] S. T. West and J. F. Wheater, Nucl. Phys. **B486**, 261 (1997).
[4] J. Boorstein and D. Kutasov, Phys. Rev. D **51**, 7111 (1995).
[5] B. Layek, A. P. Mishra, and A. M. Srivastava, Phys. Rev. D **71**, 074015 (2005).
[6] U. S. Gupta, R. K. Mohapatra, A. M. Srivastava, and V. K. Tiwari, Phys. Rev. D **82**, 074020 (2010).
[7] B. Layek, A. P. Mishra, A. M. Srivastava, and V. K. Tiwari, Phys. Rev. D **73**, 103514 (2006).
[8] A. Atreya, A. M. Srivastava, and A. Sarkar, Phys. Rev. D **85**, 014009 (2012).
[9] C. P. Korthals Altes, K.-M. Lee, and R. D. Pisarski, Phys. Rev. Lett. **73**, 1754 (1994).
[10] C. P. Korthals Altes and N. J. Watson, Phys. Rev. Lett. **75**, 2799 (1995).
[11] C. P. Korthals Altes, in *Proceedings of the XXVI International Conference on High Energy Physics, Dallas, 1992*, edited by J. R. Sanford (American Institute of Physics, New York, 1993), p. 1443.
[12] R. D. Pisarski, Phys. Rev. D **62**, 111501 (2000).
[13] A. Atreya, P. Bagchi, and A. M. Srivastava, Phys. Rev. C **90**, 034912 (2014).
[14] A. Atreya, A. Sarkar, and A. M. Srivastava, Phys. Rev. D **90**, 045010 (2014).
[15] A. V. Smilga, Ann. Phys. (N.Y.) **234**, 1 (1994).
[16] V. M. Belyaev, I. I. Kogan, G. W. Semenoff, and N. Weiss, Phys. Lett. B **277**, 331 (1992).
[17] A. Dumitru and R. D. Pisarski, Phys. Lett. B **504**, 282 (2001).
[18] A. Dumitru and R. D. Pisarski, Nucl. Phys. **A698**, 444 (2002).
[19] A. Dumitru and R. D. Pisarski, Phys. Rev. D **66**, 096003 (2002).
[20] M. Deka, S. Digal, and A. P. Mishra, Phys. Rev. D **85**, 114505 (2012).
[21] U. S. Gupta, R. K. Mohapatra, A. M. Srivastava, and V. K. Tiwari, Phys. Rev. D **86**, 125016 (2012).
[22] D. J. Gross, R. D. Pisarski, and L. G. Yaffe, Rev. Mod. Phys. **53**, 43 (1981).
[23] L. D. McLerran and B. Svetitsky, Phys. Rev. D **24**, 450 (1981).
[24] G. Boyd, J. Engels, F. Karsch, E. Laermann, C. Legeland, M. Lütgemeier, and B. Petersson, Nucl. Phys. **B469**, 419 (1996).
[25] M. Okamoto *et al.* (CP-PACS Collaboration), Phys. Rev. D **60**, 094510 (1999).
[26] K. Fukushima, Phys. Lett. B **591**, 277 (2004).
[27] A. Dumitru, D. Roder, and J. Ruppert, Phys. Rev. D **70**, 074001 (2004).
[28] V. Dixit and M. C. Ogilvie, Phys. Lett. B **269**, 353 (1991).
[29] S. Phatak, Phys. Rev. C **58**, 2383 (1998).
[30] T. M. Kalotas and A. R. Lee, Am. J. Phys. **59**, 48 (1991).